ERJ Express. Published on November 19, 2009 as doi: 10.1183/09031936.00136709

Human airway smooth muscle is structurally and mechanically similar to that of other species

Leslie YM Chin[1,4], Ynuk Bossé[4], Yuekan Jiao[4], Dennis Solomon[4], Tillie L Hackett[3,4], Peter D. Paré[2,4], and Chun Y. Seow[1,4]

[1]Departments of Pathology and Laboratory Medicine, [2]Medicine, and [3]Anesthesiology, Pharmacology and Therapeutics, [4]The James Hogg iCAPTURE Centre for Cardiovascular and Pulmonary Research, St. Paul's Hospital, University of British Columbia, Vancouver, BC, Canada

Running title: Human Airway Smooth Muscle Mechanics

Corresponding Author:
Leslie YM. Chin
iCAPTURE Centre, St. Paul's Hospital
166-1081 Burrard Street
Vancouver, BC, Canada
V6Z 1Y6
Tel: (604) 682-2344 ext. 63562
Fax: (604) 806-9274
Email: lchin@mrl.ubc.ca

This work was supported by operating grants from Canadian Institutes of Health Research (CIHR) (MOP-13271, MOP-4725). LYMC is supported by an Alexander Graham Bell Graduate Scholarship from the Natural Sciences and Engineering Research Council of Canada (NSERC). YB is supported by a fellowship from Fonds de la Recherche en Santé Québec (FRSQ) and a CIHR Strategic Training Initiative in Health Research-IMPACT fellowship. TLH is supported by a Canadian Lung Association and a CIHR Strategic Training Initiative in Health Research-IMPACT fellowship.

Abstract

Airway smooth muscle (ASM) plays a vital role in the exaggerated airway narrowing seen in asthma. However, whether asthmatic ASM is mechanically different from non-asthmatic ASM is unclear. Much of our current understanding about ASM mechanics comes from measurements made in other species. Limited data on human ASM mechanics prevents proper comparisons between healthy and asthmatic tissues as well as human and animal tissues. In the current study we sought to define the mechanical properties of healthy human ASM using tissue from intact lungs and compare these properties to measurements in other species. The mechanical properties measured included: maximal stress generation, force-length properties, the ability of the muscle to undergo length adaptation, the ability of the muscle to recover from an oscillatory strain, shortening velocity, and maximal shortening. The ultrastructure of the cells was also examined. Healthy human ASM was found to be mechanically and ultrastructurally similar to that of other species. It is capable of undergoing length adaptation and responds to mechanical perturbation like ASM from other species. Force generation, shortening capacity and velocity were all similar to other mammalian ASM. These results suggest that human ASM shares similar contractile mechanisms with other animal species and provides an important dataset for comparisons with animal models of disease and asthmatic ASM.

Key Words: asthma, airway hyperresponsiveness, ultrastructure, force-length relationship, force-velocity relationship, shortening

Introduction

While the physiological function of airway smooth muscle (ASM) is unclear [1-3], its contraction and subsequent shortening act to increase airway resistance in the lung. Asthma is characterized by episodes of increased airway resistance due to exaggerated airway narrowing. Although it is generally agreed that the narrowing is caused by ASM shortening, it is still unclear if the excessive narrowing is due to fundamental changes in the phenotype of the smooth muscle itself, or is caused by structural and/or mechanical changes in the non-contractile elements of the airway wall, or by alterations in the relationship of the airway wall to the surrounding lung parenchyma [4]. One major hurdle in determining whether ASM is truly dysfunctional in asthma is the lack of adequate data on the mechanical properties of human ASM. Much of our current knowledge about ASM contractile function has come from studies in other mammalian species, which may not adequately represent human tissue. Hence, in order to investigate a potential role for ASM in asthma it is first necessary to characterize the mechanical properties of non-asthmatic ASM. Since many hypotheses concerning the pathogenesis of asthma have been developed from animal models, it is necessary to determine the relevance of these animal models with respect to human tissues. Thus, the goal of this study was to describe the mechanical properties and ultrastructure of non-asthmatic ASM and compare the data to previous human and mammalian studies of this tissue.

In the relatively few descriptions of non-asthmatic human ASM properties, a consistent finding has been higher passive tension, lower active force (and stress), and less shortening compared with ASM preparations from other animal species [5, 6]. However

the results of these studies may be limited due to the fact that the tissues were obtained mostly from bronchial surgical resections [5-12, 32-41]. In the current study the ASM was carefully dissected from the tracheas of intact lungs donated for research.

Besides measuring the "classical" force-length and force-velocity relationships, we have focused on a newly recognized property of ASM, namely its plastic adaptability to the dynamic lung environment. None of the previous studies on mechanical properties of human ASM have studied plastic adaptation of the tissue. Importantly, in this study we used the *in situ* muscle length as the reference length for the muscle instead of the previous convention of L_{max} (the length at which force was maximal at a given instant) [13].

Materials and Methods

Tissue Preparation and Equilibration

Tracheas were removed from non-transplantable human lungs donated for research through the International Institute for the Advancement of Medicine (IIAM: Edison, NJ). All donors had no known respiratory disease and their deaths were sudden. The subject demographics and clinical details are shown in Table 1. The study was approved by the UBC-St. Paul's Hospital Ethics Committee. The whole lungs were obtained as previously described [14]. Briefly, after surgical removal the lungs were flushed with Custodiol HTK solution (Odyssey Pharmaceuticals: East Hanover, NJ) and transported by plane on ice. The average time between harvesting and arrival at the University of British Columbia was 15-20 h.

The procedure of dissection and preparation of the smooth muscle was the standard procedure for sheep tissue and has been previously described [for details see 15, 16]. Briefly, the tracheal tissue was kept at 4ºC in physiological saline solution (PSS). Dissection was undertaken within a day of obtaining the tissue. The *in situ* length of the tracheal smooth muscle was used as a reference length (L_{ref}), which was determined prior to cutting open the C-shaped cartilage ring. Connective tissue and epithelium was carefully removed to isolate a smooth muscle bundle. Muscle strips measuring 1-1.5mm wide, 0.5mm thick, and 6mm long, were attached on both ends with aluminum foil clips and mounted vertically on a force-length transducer. Before beginning the experimental protocol, the muscle was equilibrated at L_{ref} by periodic electrical field stimulation (EFS) at 5-minute intervals for a period of 1.5h. Since some tissues exhibited substantial leukotriene-mediated tone without extrinsic stimulation, the CysLT1 receptor antagonist montelukast (10^{-6} M) was added to the PSS for all of the experiments, which prevented or eliminated tone.

Mechanical Measurements

After equilibration, the maximal isometric force produced in response to EFS at L_{ref} was determined (herein called F_{max}). For the force-length relationship the muscle was either stretched or shortened in a step-wise fashion as previously described [15, 17] and allowed to adapt to every new length for 20 minutes during which it was stimulated with EFS at 5-minute intervals. Five different lengths were examined: 0.5, 0.75, 1.0, 1.25, and 1.5 L_{ref}. To determine the response to length perturbation, a 10 minute, 0.2Hz, 30% L_{ref} length

oscillation was applied. The recovery of EFS-induced (active) force was followed for 30 minutes after oscillation by stimulating with EFS at 5-minute intervals. For the force-velocity curves, velocity measurements were made after release (quick switch from isometric to isotonic contraction) at five graded loads (between zero and F_{max}) at L_{ref} as previously described [18]. Velocities were measured at two time points: one at the peak of tetanic force and one mid-way to the peak. This is due to the non-linear nature of shortening velocity, which peaks early on as developed force reaches ~50% of F_{max}, and settles to a lower plateau after the force reaches F_{max} [19]. Shortening velocity against a given load was recorded 100 msec after the release, during the steady-phase of shortening. The curves were fit using Hill's hyperbolic equation [20]. Maximal isotonic shortening was established by allowing a muscle to contract against a preload equal to 10% and 20% F_{max}. It was not possible to perform the shortening at zero-load because the servo-system of the myograph became unstable at low loads. Therefore, the maximal shortening was extrapolated to zero load from these two points.

Histology and Electron Microscopy

At the end of the mechanical protocols the tissue preparations were fixed at L_{ref} in 10% formalin for histology or a formaldehyde cocktail for transmission electron microscopy (EM). The histology was performed as previously described [21]. The amount of muscle in the preparation was determined by staining transverse sections with Masson's trichrome and quantified by manual tracing using Image ProPlus 4.5 (MediaCybernetics: Bethesda, MD). Maximal stress generating capacity was determined by dividing F_{max} (in mN) by the

cross-sectional area (in mm^2) of muscle present in the preparation. The protocol for EM followed the standard procedure previously described in our lab (see [23] for details).

Statistical Analysis

Force and length measurements were normalized to F_{max} or L_{ref} respectively and expressed as fractions of F_{max} and L_{ref}. Velocity of shortening was expressed as L_{ref}/sec. Aggregate data were expressed as mean ± SEM. ANOVA and regression analyses were accomplished using GraphPad Prism 5 (GraphPad Software, Inc.: La Jolla, CA). $p \leq 0.05$ was considered to be sufficient to reject the null hypothesis.

Results

Muscle bundle properties and morphology

Human lungs were received from six donors with an average age of 25.8±2.8 years. After measurements of mechanical properties, muscle strips were fixed and stained with Masson's Trichrome for histological morphometry (n = 4). From the histological sections the cross-sectional area of the muscle was measured and compared to the entire tissue preparation (Fig. 1A). The percentage of smooth muscle cross-sectional area to the total cross-sectional area of the tissue preparation averaged 36.5±0.04%. The maximal stress generated by the muscle averaged 82.1±17.3 mN/mm^2.

Ultrastructure

Muscle strips were also fixed for EM. A transverse electron micrograph of a muscle cell is shown in Figure 1B. The cells are similarly 'packed' within bundles like ASM from other species (Fig. 1B), and share similar intracellular features. Like other mammalian ASM

cells, human cells lack the well-organized arrays of contractile filaments seen in striated muscle (Fig. 1B and 1C). Myosin thick filaments are present throughout the cell and are vastly outnumbered by actin filaments (Fig. 1B and 1C). Areas of electron dense material, known as dense bodies and plaques, are also seen. Mitochondria, sarcoplasmic reticula, caveolae, and microtubules are also present and are indistinguishable from their counterparts in animal cells.

Force-Length Properties and Length Adaptation

The relationship between muscle length and force generating capacity was examined by recording force at five different lengths (Fig. 2). Between shorter and longer lengths the muscle was returned to L_{ref} and re-equilibrated (Fig 2A). Immediately following a length change from L_{ref}, the active force declined and gradually recovered to a greater force over time (Fig. 2B). On average, the active force did not fully recover to F_{max} at any of the lengths during the 20 minutes. Part of the incomplete recovery was due to a general force deterioration over the time course of the experiment. Correction for force deterioration was accomplished by assuming a linear decline and fitting a line through the first contraction at L_{ref} and the last (fifth) contraction after the length was returned to L_{ref} (force = -0.0006 x time + 1, where time is in minutes; suggesting an average decline of 10.8% from initial force after 3h). This correction assumes that force at L_{ref} returns to F_{max} in the absence of deterioration, thus preventing an underestimation of force recovery (corrected values are presented in Figs. 2 and 3). To compare the extent of length adaptation, the initial force after a length change (first contraction) was compared to the final force measurement after the adaptation period (fifth contraction), this is displayed in Figure 3.

There was a significant length adaptation of active force over the 20 minute period (Fig. 3) (ANOVA: $p<0.0001$). Bonferroni posttests demonstrated that active force at $0.50xL_{ref}$ and $1.50xL_{ref}$ were significantly greater after the period of adaptation ($p<0.05$ and $p<0.001$, respectively). Passive force (Fig. 2C and 3) also demonstrated a significant length adaptation (ANOVA: $p=0.0053$). At lengths longer than L_{ref}, the passive force initially increased with the length change but decreased over the period of adaptation. Conversely, at shorter lengths, the passive force initially declined but gradually increased over the 20 minute period. On average the passive force did not reach pre-length change levels despite significant adaptation (Fig. 3).

Recovery from Mechanical Perturbation

The magnitude and time required for force recovery following a perturbation was examined by applying an oscillatory strain to the relaxed muscle. The ten minute length oscillation occurred at a frequency that mimics human breathing (0.2Hz) and at a magnitude similar to deep inspiration (30% L_{ref}). As seen in Figure 4 (not corrected for force deterioration), immediately following oscillation the force decreased to 0.643 ± 0.03 F_{max} and recovered to 0.953 ± 0.03 F_{max} 30 minutes after oscillation.

Shortening Velocity

Two sets of data were generated to examine the shortening velocity of human ASM. At both time points, the muscle was released to five different pre-determined loads (each representing a certain percentage of F_{max}). The difference between the two sets of data was the time of release (Fig. 5). The late releases were performed during the tetanic plateau of

active force while the early releases were performed mid-way to the plateau (on average between 3 to 4 seconds after the onset of stimulation). Both data sets were fitted with Hill's hyperbolic equation [20]. Maximal shortening velocity (V_{max}) determined by Hill's equation was 0.609 and 0.394 L_{ref}/s for the early and late-phase, respectively. Force-velocity curves at the two time points were significantly different (repeated measures ANOVA: $p<0.0001$).

Maximal Isotonic Shortening

In four muscle preparations the extent of unloaded shortening was determined (Fig. 7). Each ASM strip was allowed to isotonically shorten against a predetermined load (10% and 20% F_{max}). The maximal unloaded shortening was extrapolated from a linear regression of the points (R^2=0.749, p=0.0055). This regression assumes that the ascending limb of the force-length curve for a non-adapted muscle is linear [25]. The 95% confidence intervals ranged from 60.3 to 84.1% of shortening at zero-load with an average of 72.2% (total length of the muscle).

Discussion

Despite the prominent role of ASM in airway diseases, the basic mechanical properties of human ASM have not been adequately determined. This study is the most comprehensive description of the mechanical properties of human ASM to-date and is unique in that the experiments were performed within the paradigm of ASM mechanical plasticity using a high quality tissue source. Our results demonstrate that human ASM possesses similar mechanical properties and morphological features as those found in other mammals such

as dogs, pigs, and sheep. This provides justification for using ASM tissues from non-human species to elucidate contractile mechanisms. Also, mechanical responses to experimental interventions in non-human mammalian ASM can now be justifiably interpreted in terms of human airway physiology. This study also provides a database of mechanical parameters for intact non-asthmatic human ASM, an invaluable reference against which asthmatic ASM can be compared.

Qualitatively, human ASM is indistinguishable from that of other species, as concluded from comparisons with ultrastructural images [15, 22, 25, 29]. The present study demonstrates the feasibility of quantitative comparisons of ultrastructural features (e.g. filament densities) and the relative abundance of mitochondria, caveolae, sarcoplasmic reticula, and other organelles of interest. Comparisons of these features will provide invaluable insights into the phenotypic changes associated with asthmatic ASM.

The results of previous studies suggested that human ASM possesses reduced stress generating capacity, reduced shortening capacity, and greater passive stiffness compared to other species [5, 6]. Human ASM was found to generate a maximal stress of 50±20 mN/mm^2 compared to 140, 72, and 80 mN/mm^2 in rabbit, dog, and swine ASM, respectively [6]. The present results show that human ASM (82 ±17.3 mN/mm^2) generates stress which is comparable to dog and swine ASM. Another major finding of the present study is the ability of human ASM to undergo extensive shortening (72%) (Fig. 7). This degree of shortening is similar to the reported values in other animal species which range from 61 to 71%, and is much greater than the previously reported human ASM value of

25±9.0% [6]. This discrepancy could be related to the reduced stress generated by the tissues in earlier studies which were dissected from bronchi obtained from surgical resections. In addition, the starting length of the muscle was set at L_{max}, an arbitrary length that is greatly influenced by the state of adaptation of the muscle [13].

Another difference in the present study, which could influence the degree of maximal shortening, was the percentage of muscle to total tissue area (36.49±0.04%) which is much greater than the 8.7% reported in preparations from earlier human studies [5]. These data suggest that the previously studied human ASM was surrounded by a greater proportion of connective tissue resulting in higher passive stiffness, when compared with other species. Increased connective tissue could also prevent shortening by acting as a radial constraint and/or compressive load in parallel to the muscle cells [28]. This hypothesis is supported by the observation that treating human ASM preparations with collagenase, led to a 50% increase in maximal isotonic shortening [11, 12]. Our carefully dissected tracheal preparations had similar ASM content to other non-human preparations which ranged from 25-35% smooth muscle area [6]. While the decreased connective tissue surrounding the muscle may have increased shortening in our study, it is unclear if passive tension was affected. In the previous study conducted at L_{max}, the passive tension in the muscle preparation was 60±8.8% of maximal force [5]. In the present study average passive tension at L_{ref} was 22.4±0.1% F_{max}.

Shortening velocity in smooth muscle peaks early in contraction before force reaches a plateau; the velocity then decreases to a lower level after force plateaus and this velocity is

maintained during the sustained phase of contraction. This decrease in velocity has been attributed to the development of latch-bridges caused by dephosphorylation of the myosin regulatory light chain in arterial muscle [26]. In non-human ASM, it has been proposed that the decreased velocity is likely due to thick filament lengthening during force development [18] and myosin phosphorylation was not found to correlate to velocity [27]. The present finding that velocity declines (Fig. 6) during the time course of an isometric contraction suggests that myosin filaments in human ASM undergo similar rearrangements.

This is the first study to investigate whether length adaptation occurs in human ASM. Smooth muscle like striated muscle operates over a length range. In striated muscle the force-length relationship is characterized by a well-defined optimal length where developed force is at its maximum. Outside the narrow plateau of maximal force, the force developed by the muscle decreases at shorter and longer lengths. This relationship depends on the overlap of the actin and myosin filaments within the muscle. Likewise, smooth muscle displays a force-length relationship that approximately resembles a concave-down parabolic curve. However, airway smooth muscle producing 'suboptimal' force at a shorter or longer length can adapt to the new length, increasing its force within minutes [17]. This requires rearrangement of contractile and cytoskeletal proteins, and effectively broadens the force-length relationship of the smooth muscle [24, 29]. Thus, length adaptation allows smooth muscle to operate over the large length ranges seen *in vivo,* particularly in the smooth muscle tissues that line hollow organs that undergo large volume changes. Compared to previous studies in canine ASM [17] our data suggests that

human ASM is less adaptable, that is, the length range of the force plateau in human ASM is smaller than that of canine ASM. Nevertheless, maximal force in human ASM is length-independent over the range of 0.75 - 1.5 L_{ref} (ANOVA, $p<0.05$), a clear sign that human ASM is capable of length adaptation (Fig. 3).

The ability of the muscle to undergo length adaptation suggests that human ASM is capable of the mechanical plasticity demonstrated in other mammalian species. This ability to rearrange intracellular elements to generate force is further supported by the muscle's response to length oscillation (Fig. 4). Our laboratory has previously shown in swine tissue that an oscillatory strain causes a decrease in force immediately after oscillation, followed by an exponential force recovery that coincides with myosin filament reformation [23]. However, the magnitude of recovery is somewhat blunted in human ASM since the force did not fully recover to F_{max}, as it does in swine. Likewise, the rate of recovery is slower, with a rate constant of 0.139 s^{-1} versus 0.234 s^{-1} in swine ASM [23]. Human ASM is also more easily perturbed, since the force produced by human ASM immediately after oscillation was 64% F_{max} compared to ~79% F_{max} in swine [23]. This implies that human ASM has a more labile intracellular structure that reorganizes slower than ASM from other species. *In vivo,* this may be beneficial for maintenance of airway patency. Coupled with its reduced ability to undergo length adaptation, the force loss associated with oscillation could enhance and prolong the effectiveness of bronchoprotection provided by a deep inspiration [30-31]. The increased sensitivity to mechanical perturbation could be related to differences in the muscle's contractile apparatus or due to differences in extracellular structures, perhaps exposing human ASM

to greater internal forces than is seen by other species. Comparisons to ASM from asthmatic subjects are certainly needed.

Previous studies comparing asthmatic and non-asthmatic ASM mechanical properties have suggested increased contractility (force development or shortening) [12, 39, 41] or sensitivity to certain agonists in asthmatic ASM [12, 32, 36], while others have shown no differences [33-35, 37, 38, 40]. With respect to the current study, it is unclear whether these are true differences or due to the inexactness of using L_{max} to determine 'optimal force,' since the velocity, extent of shortening, and sensitivity to an agonist [42] are all length dependent. Only two studies have normalized force to cross-sectional muscle area, concluding that asthmatics generate more stress than non-asthmatics [12, 41]. Based on the results of the present study we suggest that these investigators may have underestimated maximal stress and the extent of shortening, either because of the way L_{max} was determined or due to less than optimal tissue quality. However these factors may have equally affected asthmatics and non-asthmatics and thus would not alter their conclusions. Alternatively, it is possible that these factors could differentially affect asthmatic and non-asthmatic tissues and lead to (or conceal) differences between the two groups.

In conclusion, this study is the first comprehensive study of the mechanical properties of healthy human ASM sourced from an intact lung. We have demonstrated that human ASM has ultrastructural features and mechanical properties which are similar to other animal species and is capable of length adaptation. These results suggest that human ASM

likely has the same intracellular organization and undergoes the same processes of mechanical plasticity that have been identified in the ASM of other species.

References

1. Seow CY and Fredberg JJ. Historical perspective on airway smooth muscle: the saga of a frustrated cell. *J.Appl.Physiol.* 2001; 91: 2: 938-952.

2. Mead J. Point: airway smooth muscle is useful. *J.Appl.Physiol.* 2007; 102: 4: 1708-9; discussion 1710.

3. Fredberg JJ. Counterpoint: airway smooth muscle is not useful. *J.Appl.Physiol.* 2007; 102: 4: 1709-10; discussion 1710-1.

4. An SS, Bai TR, Bates JH, Black JL, Brown RH, Brusasco V, Chitano P, Deng L, Dowell M, Eidelman DH, Fabry B, Fairbank NJ, Ford LE, Fredberg JJ, Gerthoffer WT, Gilbert SH, Gosens R, Gunst SJ, Halayko AJ, Ingram RH, Irvin CG, James AL, Janssen LJ, King GG, Knight DA, Lauzon AM, Lakser OJ, Ludwig MS, Lutchen KR, Maksym GN, Martin JG, Mauad T, McParland BE, Mijailovich SM, Mitchell HW, Mitchell RW, Mitzner W, Murphy TM, Paré PD, Pellegrino R, Sanderson MJ, Schellenberg RR, Seow CY, Silveira PS, Smith PG, Solway J, Stephens NL, Sterk PJ, Stewart AG, Tang DD, Tepper RS, Tran T, Wang L. Airway smooth muscle dynamics: a common pathway of airway obstruction in asthma. *Eur.Respir.J.* 2007; 29: 5: 834-860.

5. Ishida K, Paré PD, Hards J, Schellenberg RR. Mechanical properties of human bronchial smooth muscle in vitro. *J.Appl.Physiol.* 1992; 73: 4: 1481-1485.

6. Opazo Saez AM, Schellenberg RR, Ludwig MS, Meiss RA, Paré PD. Tissue elastance influences airway smooth muscle shortening: comparison of mechanical properties among different species. *Can.J.Physiol.Pharmacol.* 2002; 80: 9: 865-871.

7. De Jongste J, Mons H, Van Strik R, Bonta I, Kerrebijn K. Human small airway smooth muscle responses in vitro; actions and interactions of methacholine, histamine and leukotriene C4. *Eur.J.Pharmacol.* 1986; 125: 1: 29-35.

8. De Jongste JC, Mons H, Block R, Bonta IL, Frederiksz AP, Kerrebijn KF. Increased in vitro histamine responses in human small airways smooth muscle from patients with chronic obstructive pulmonary disease. *Am.Rev.Respir.Dis.* 1987; 135: 3: 549-553.

9. de Jongste JC, van Strik R, Bonta IL, Kerrebijn KF. Measurement of human small airway smooth muscle function in vitro with the bronchiolar strip preparation. *J.Pharmacol.Methods* 1985; 14: 2: 111-118.

10. Jongejan RC, de Jongste JC, van Strik R, Raatgeep HR, Bonta IL, Kerrebijn KF. Measurement of human small airway smooth muscle function in vitro. Comparison of bronchiolar strips and segments. *J.Pharmacol.Methods* 1988; 20: 2: 135-142.

11. Bramley AM, Roberts CR, Schellenberg RR. Collagenase increases shortening of human bronchial smooth muscle in vitro. *Am.J.Respir.Crit.Care Med.* 1995; 152: 5 Pt 1: 1513-1517.

12. Bramley AM, Thomson RJ, Roberts CR, Schellenberg RR. Hypothesis: excessive bronchoconstriction in asthma is due to decreased airway elastance. *Eur.Respir.J.* 1994; 7: 2: 337-341.

13. Bai TR, Bates JH, Brusasco V, Camoretti-Mercado B, Chitano P, Deng LH, Dowell M, Fabry B, Ford LE, Fredberg JJ, Gerthoffer WT, Gilbert SH, Gunst SJ, Hai CM, Halayko AJ, Hirst SJ, James AL, Janssen LJ, Jones KA, King GG, Lakser OJ, Lambert RK, Lauzon AM, Lutchen KR, Maksym GN, Meiss RA, Mijailovich SM, Mitchell HW, Mitchell RW, Mitzner W, Murphy TM, Paré PD, Schellenberg RR, Seow CY, Sieck GC,

Smith PG, Smolensky AV, Solway J, Stephens NL, Stewart AG, Tang DD, Wang L. On the terminology for describing the length-force relationship and its changes in airway smooth muscle. *J.Appl.Physiol.* 2004; 97: 6: 2029-2034.

14. Hackett TL, Shaheen F, Johnson A, Wadsworth S, Pechkovsky DV, Jacoby DB, Kicic A, Stick SM, Knight DA. Characterization of side population cells from human airway epithelium. *Stem Cells* 2008; 26: 10: 2576-2585.

15. Ali F, Chin L, Paré PD, Seow CY. Mechanism of partial adaptation in airway smooth muscle after a step change in length. *J.Appl.Physiol.* 2007; 103: 2: 569-577.

16. Bossé Y, Chin LY, Paré PD, Seow CY. Adaptation of Airway Smooth Muscle to Basal Tone: Relevance to Airway Hyperresponsiveness. *Am.J.Respir.Cell Mol.Biol.* 2008.

17. Pratusevich VR, Seow CY, Ford LE. Plasticity in canine airway smooth muscle. *J.Gen.Physiol.* 1995; 105: 1: 73-94.

18. Seow CY, Pratusevich VR, Ford LE. Series-to-parallel transition in the filament lattice of airway smooth muscle. *J.Appl.Physiol.* 2000; 89: 3: 869-876.

19. Seow CY and Stephens NL. Force-velocity curves for smooth muscle: analysis of internal factors reducing velocity. *Am.J.Physiol.* 1986; 251: 3 Pt 1: C362-8.

20. Hill AV. The heat of shortening and the dynamic constants of muscle. 1938; 126: 136-195.

21. Syyong H, Cheung C, Solomon D, Seow CY, Kuo KH. Adaptive response of pulmonary arterial smooth muscle to length change. *J.Appl.Physiol.* 2008; 104: 4: 1014-1020.

22. Herrera AM, Martinez EC, Seow CY. Electron microscopic study of actin polymerization in airway smooth muscle. *Am.J.Physiol.Lung Cell.Mol.Physiol.* 2004; 286: 6: L1161-8.

23. Kuo KH, Wang L, Paré PD, Ford LE, Seow CY. Myosin thick filament lability induced by mechanical strain in airway smooth muscle. *J.Appl.Physiol.* 2001; 90: 5: 1811-1816.

24. Gunst SJ, Meiss RA, Wu MF, Rowe M. Mechanisms for the mechanical plasticity of tracheal smooth muscle. *Am.J.Physiol.* 1995; 268: 5 Pt 1: C1267-76.

25. Herrera AM, McParland BE, Bienkowska A, Tait R, Paré PD, Seow CY. 'Sarcomeres' of smooth muscle: functional characteristics and ultrastructural evidence. *J.Cell.Sci.* 2005; 118: Pt 11: 2381-2392.

26. Dillon PF, Aksoy MO, Driska SP, Murphy RA. Myosin phosphorylation and the cross-bridge cycle in arterial smooth muscle. *Science* 1981; 211: 4481: 495-497.

27. Mitchell RW, Seow CY, Burdyga T, Maass-Moreno R, Pratusevich VR, Ragozzino J, Ford LE. Relationship between myosin phosphorylation and contractile capability of canine airway smooth muscle. *J.Appl.Physiol.* 2001; 90: 6: 2460-2465.

28. Paré PD, McParland BE, Seow CY. Structural basis for exaggerated airway narrowing. *Can.J.Physiol.Pharmacol.* 2007; 85: 7: 653-658.

29. Kuo KH, Herrera AM, Wang L, Paré PD, Ford LE, Stephens NL, Seow CY. Structure-function correlation in airway smooth muscle adapted to different lengths. *Am.J.Physiol.Cell.Physiol.* 2003; 285: 2: C384-90.

30. Skloot G, Permutt S, Togias A. Airway hyperresponsiveness in asthma: a problem of limited smooth muscle relaxation with inspiration. *J.Clin.Invest.* 1995; 96: 5: 2293-403.

31. Moore BJ, Verburgt LM, King GG, Paré PD. The effect of deep inspiration on methacholine dose-response curves in normal subjects. *Am.J.Respir.Crit.Care.Med.* 1997; 156: 4: 1278-81.

32. Schellenberg RR and Foster A. In vitro responses of human asthmatic airway and pulmonary vascular smooth muscle. *Int.Arch.Allergy Appl.Immunol.* 1984; 75: 3: 237-241.

33. Roberts JA, Raeburn D, Rodger IW, Thomson NC. Comparison of in vivo airway responsiveness and in vitro smooth muscle sensitivity to methacholine in man. *Thorax* 1984; 39: 11: 837-843.

34. Cerrina J, Le Roy Ladurie M, Labat C, Raffestin B, Bayol A, Brink C. Comparison of human bronchial muscle responses to histamine in vivo with histamine and isoproterenol agonists in vitro. *Am.Rev.Respir.Dis.* 1986; 134: 1: 57-61.

35. Goldie RG, Spina D, Henry PJ, Lulich KM, Paterson JW. In vitro responsiveness of human asthmatic bronchus to carbachol, histamine, beta-adrenoceptor agonists and theophylline. *Br.J.Clin.Pharmacol.* 1986; 22: 6: 669-676.

36. de Jongste JC, Mons H, Bonta IL, Kerrebijn KF. In vitro responses of airways from an asthmatic patient. *Eur.J.Respir.Dis.* 1987; 71: 1: 23-29.

37. Whicker SD, Armour CL, Black JL. Responsiveness of bronchial smooth muscle from asthmatic patients to relaxant and contractile agonists. *Pulm.Pharmacol.* 1988; 1: 1: 25-31.

38. Cerrina J, Labat C, Haye-Legrande I, Raffestin B, Benveniste J, Brink C. Human isolated bronchial muscle preparations from asthmatic patients: effects of indomethacin and contractile agonists. *Prostaglandins* 1989; 37: 4: 457-469.

39. Bai TR. Abnormalities in airway smooth muscle in fatal asthma. *Am.Rev.Respir.Dis.* 1990; 141: 3: 552-557.

40. Bai TR. Abnormalities in airway smooth muscle in fatal asthma. A comparison between trachea and bronchus. *Am.Rev.Respir.Dis.* 1991; 143: 2: 441-443.

41. Thomson RJ, Bramley AM, Schellenberg RR. Airway muscle stereology: implications for increased shortening in asthma. *Am.J.Respir.Crit.Care Med.* 1996; 154: 3 Pt 1: 749-757.

42. Bosse Y, Chin LY, Pare PD, Seow CY. Chronic Activation in Shortened Airway Smooth Muscle: A Synergistic Combination Underlying Airway Hyperresponsiveness? *Am.J.Respir.Cell Mol.Biol.* 2009; .

Figure Legends

Figure 1. **Morphology and ultrastructure of the airway smooth muscle**
A) ASM strips were stained with Masson's Trichrome. The smooth muscle is red, connective tissue blue, and nuclei black. The yellow outline encircles the muscle bundles. The glandular, red staining cells were excluded. Morphometric analysis was used to determine the cross-sectional area of muscle in the dissected strip. This area was used to calculate the maximal stress generated by each smooth muscle preparation (stress = force/cross sectional area). Color segmentation was used to exclude the blue connective tissue within muscle bundles. Image width = 1.14 mm. B) An electron micrograph of a ASM cell sectioned transversally. Arrowheads indicate dense bodies (cytoplasmic) and dense plaques (membrane associated). White arrows indicate intermediate filaments; white arrowheads indicate microtubules. M: Mitochondria; Ca: Caveolae; SR: Sarcoplasmic reticulum; BL: Basal lamina; Co: Collagen fibers. Inset: Magnification of the square shown in B. Small arrows indicate actin thin filaments and larger arrows indicate myosin thick filaments. Bar = 0.5 μm. C) Electron micrograph of a longitudinal ASM cell section. Arrowheads point to dense bodies and arrows point to myosin filaments. Bar = 0.5 μm.

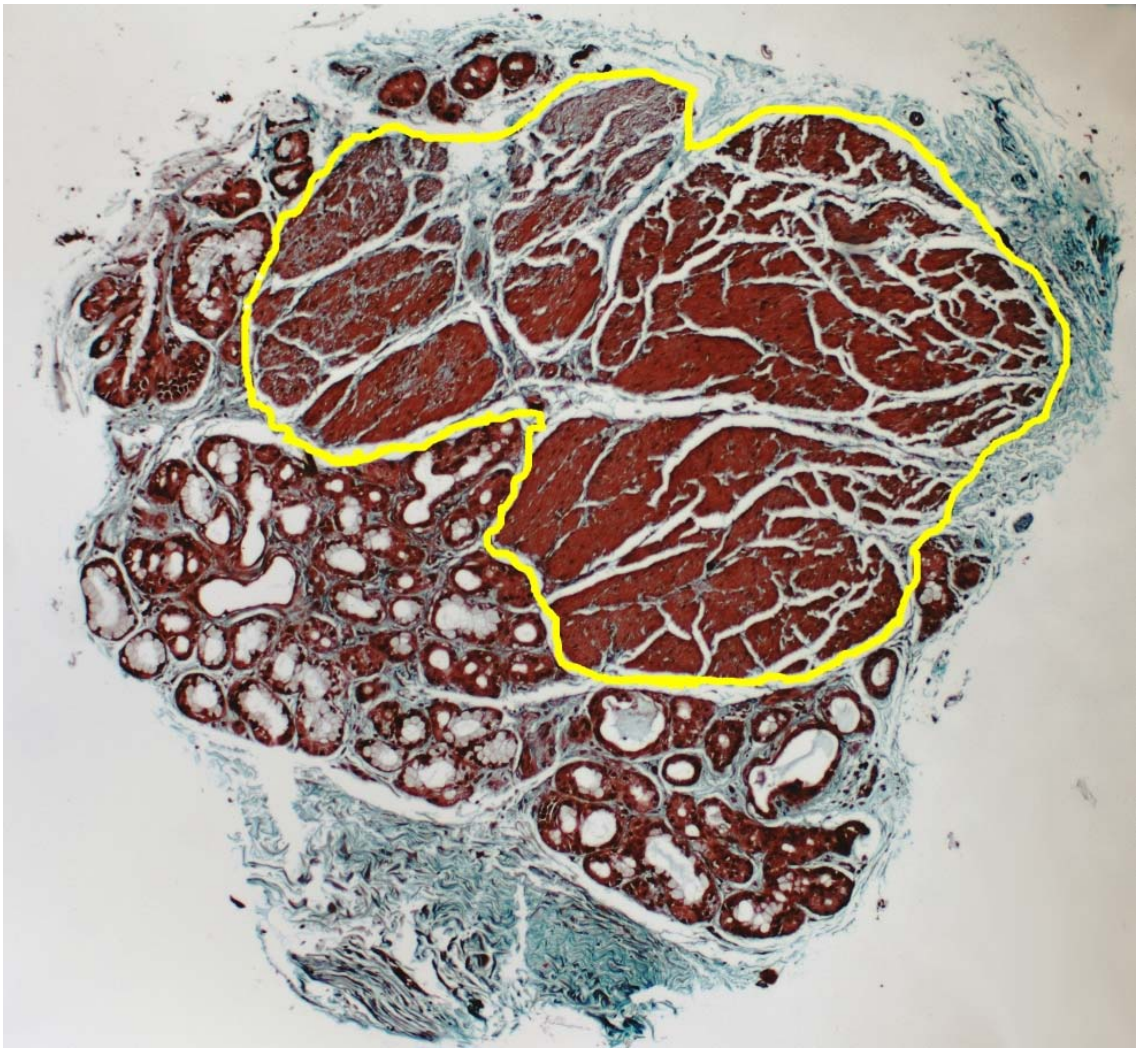

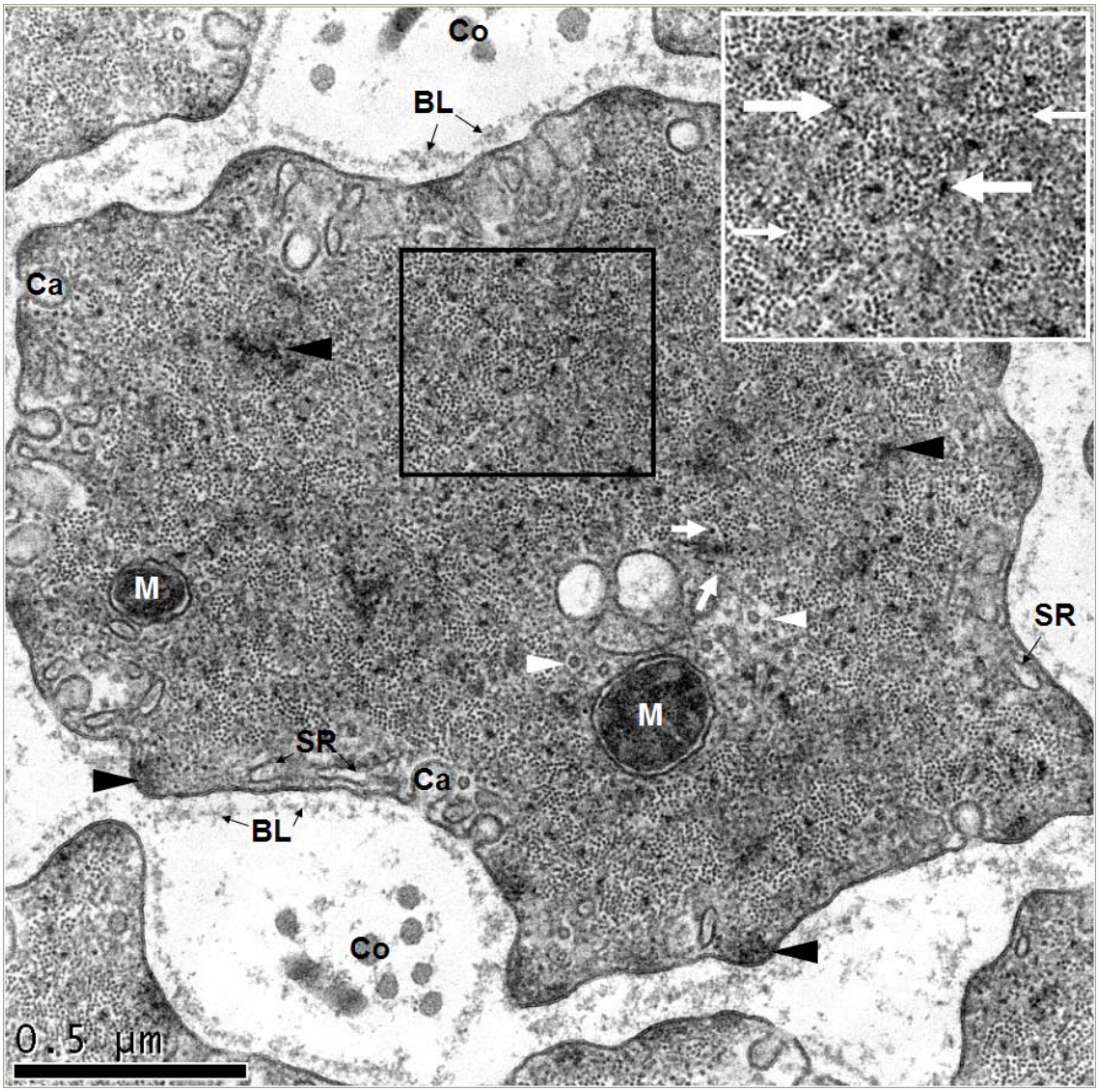
Co
BL
Ca
M
SR
M
SR
Ca
BL
Co
0.5 µm

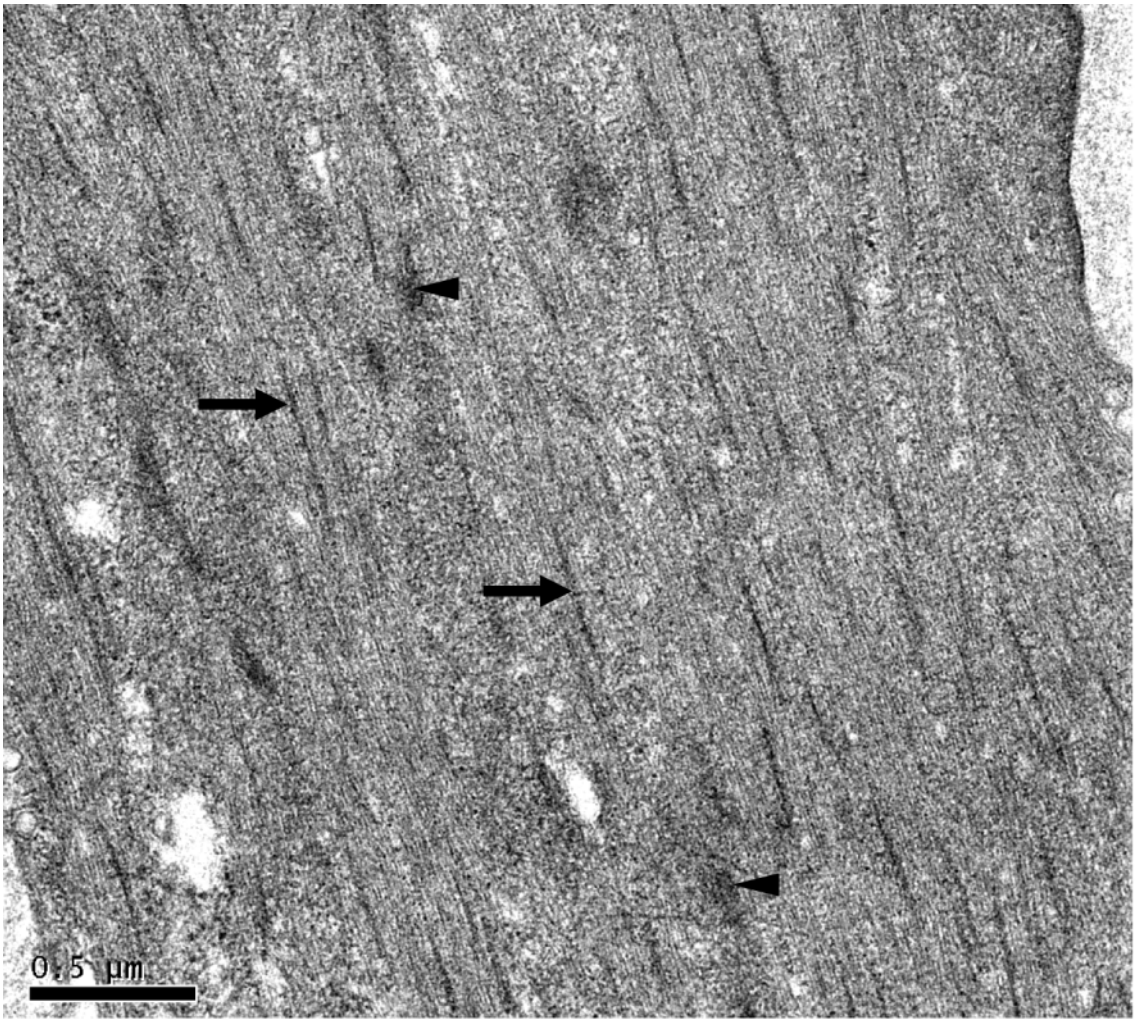

Figure 2. **Isometric force at different lengths**
A) The sequence and the time course of length changes are shown. ASM strips were either shortened or lengthened in the relaxed state to 0.50, 0.75, 1.25 or 1.50 L_{ref}. The muscle was stimulated to contract 5 times with EFS at 5-minute intervals after every length change. The force was corrected for force deterioration over time (see text for details). Between shortening and lengthening steps, the muscle was returned to, and readapted at, L_{ref}. Grey hexagons indicate the time points where EFS occurred. The active force (B) and passive force (C) were recorded at every contraction. Error bars indicate SEM, n=6 from 6 different donors.

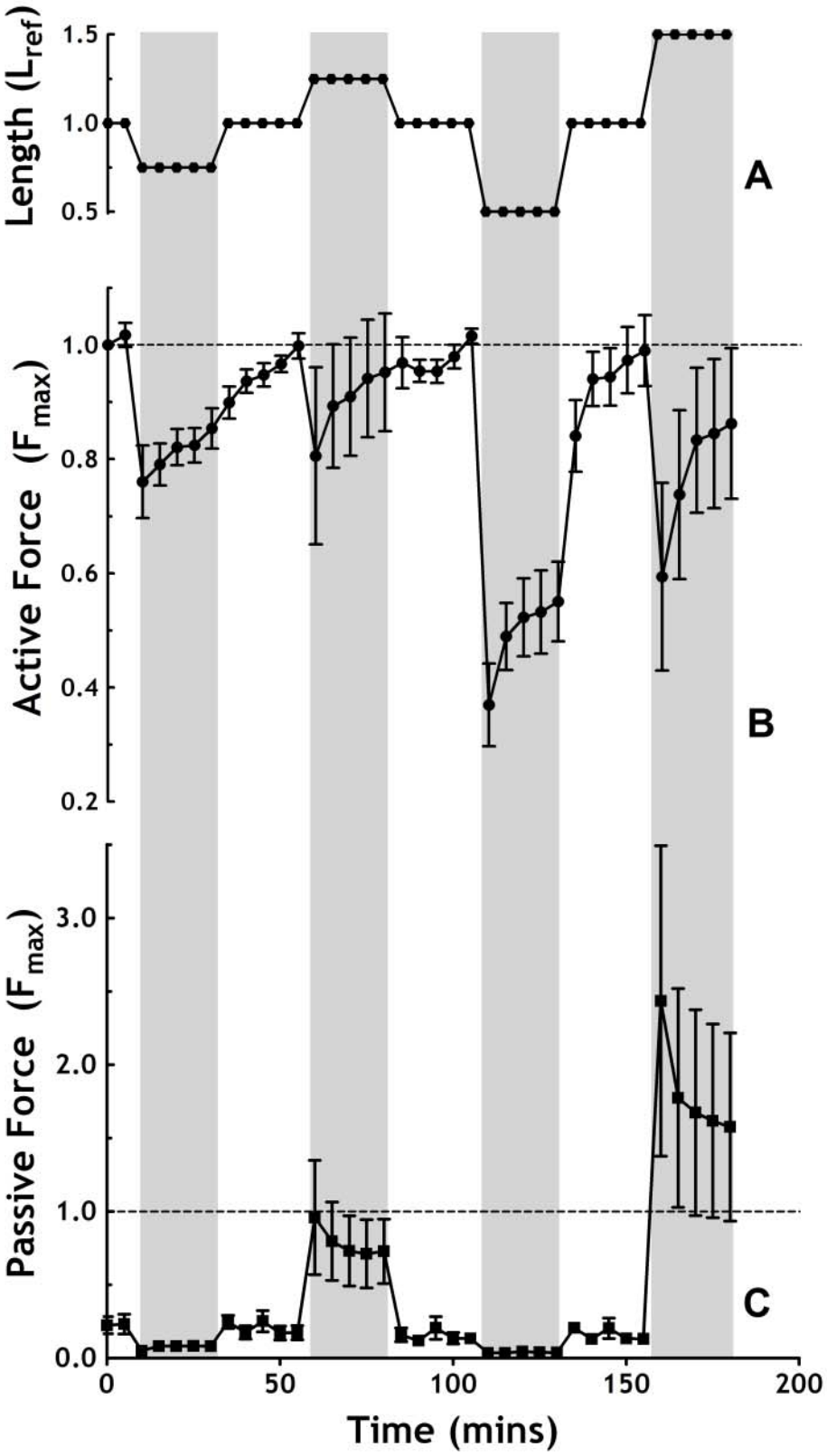
Length (L_{ref})
1.5
1.0
0.5
A
Active Force (F_{max})
1.0
0.8
0.6
0.4
0.2
B
Passive Force (F_{max})
3.0
2.0
1.0
0.0
C
0
50
100
150
200
Time (mins)

Figure 3. **Active and passive force-length relationships before and after length adaptation**

From L_{ref}, the ASM strips were either shortened or lengthened to 0.50, 0.75, 1.25, and 1.50 L_{ref} (refer to Fig. 2 for sequence and time course of length changes and stimulation). Active force (circles) and passive force (squares) both before (solid lines and closed symbols) and after (dashed lines and open symbols) length adaptation are shown. The force was corrected for deterioration over the time period of the experiment, see text for details. Active force before and after adaptation was length independent in the range 0.75-1.5 L_{ref} (ANOVA, $p<0.05$). Error bars indicate SEM, n=6 from 6 different donors. *: $p<0.05$, **: $p<0.01$, ***: $p<0.001$; adapted force compared to non-adapted force at a given length.

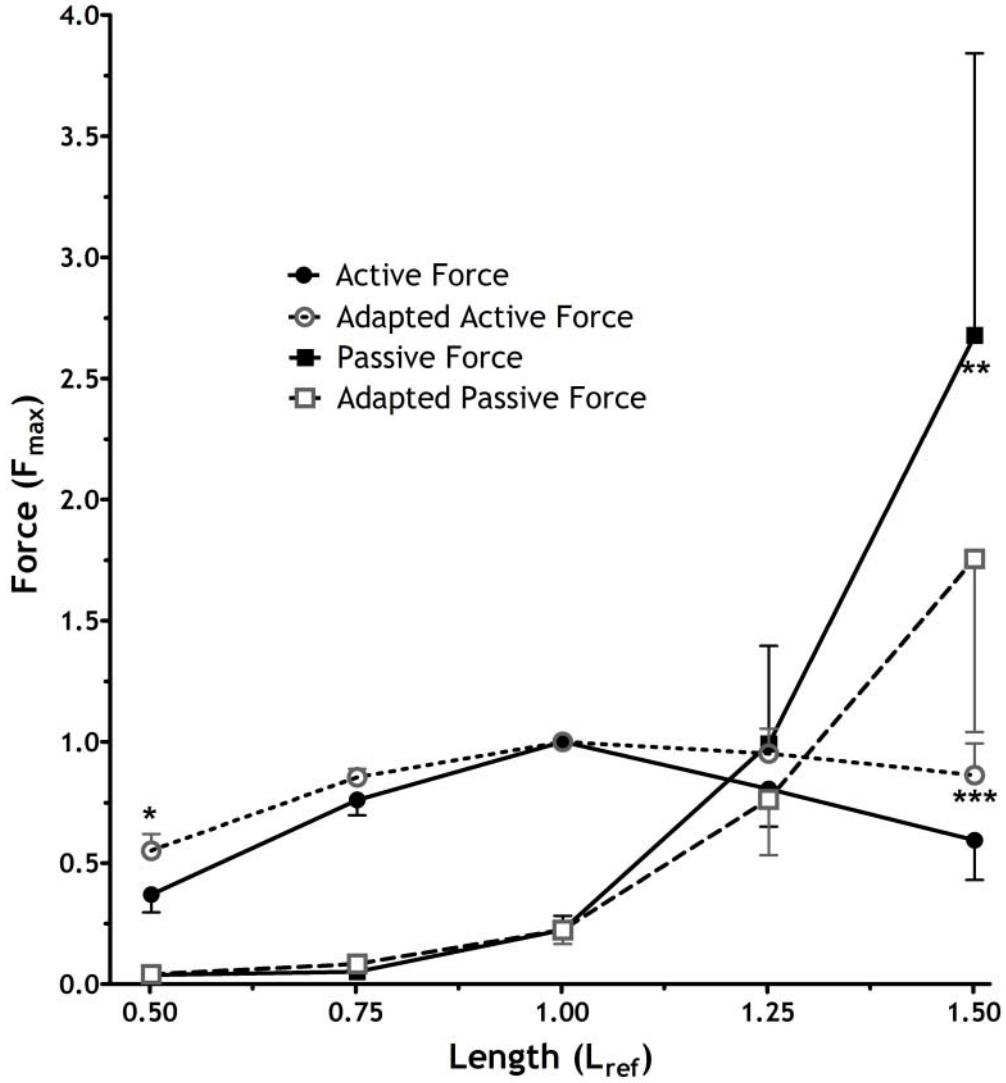

***Figure 4*. Isometric force recovery following a length oscillation**
Recovery of isometric force following a ten-minute, 0.2Hz, 30% L_{ref} length oscillation. ASM strips were adapted to L_{ref} prior the oscillation. The force produced by seven EFS-induced contractions were recorded at 5-minute intervals following the oscillation. Error bars indicate SEM, n=6, R^2=0.7254.

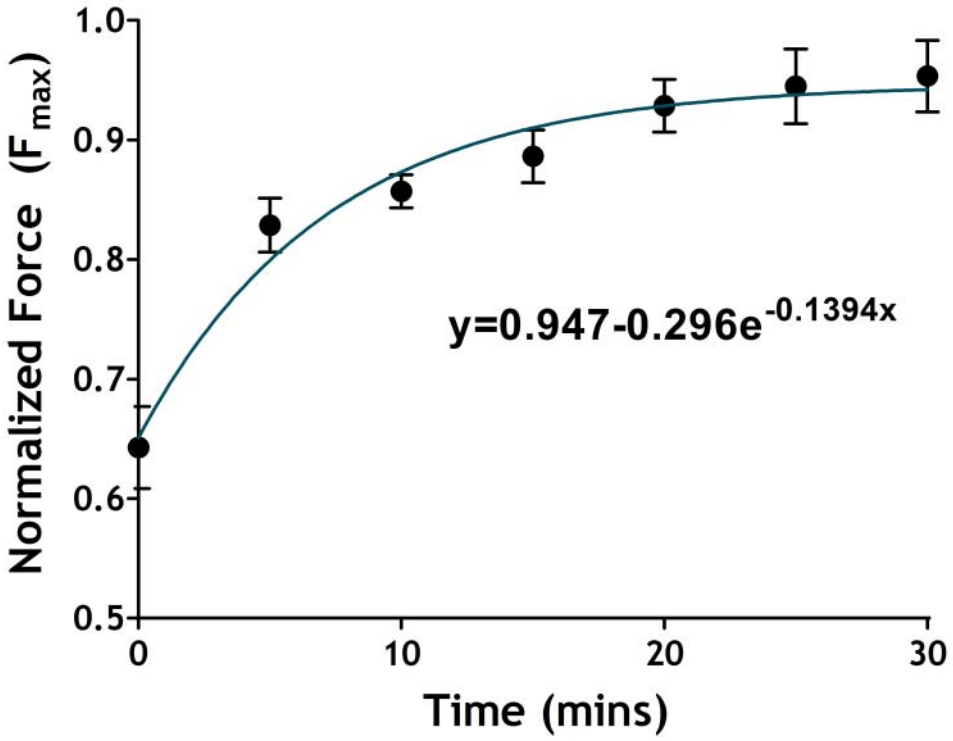

***Figure 5.* Determining shortening velocity during an isotonic contraction**
Shortening velocity was determined at two time points during EFS (A and B). A late load release was performed during the force plateau (A), while an early load release was performed midway to the force plateau (B). The top panel shows representative traces of force and length records of an isotonic release. The load against which the muscle contracted was reduced to a specific load in a time space of 10 ms (6 mN in the case shown here). The velocity was determined by calculating the slope of the tangent line during steady-state shortening at 100 ms. For each release, five different loads were used.

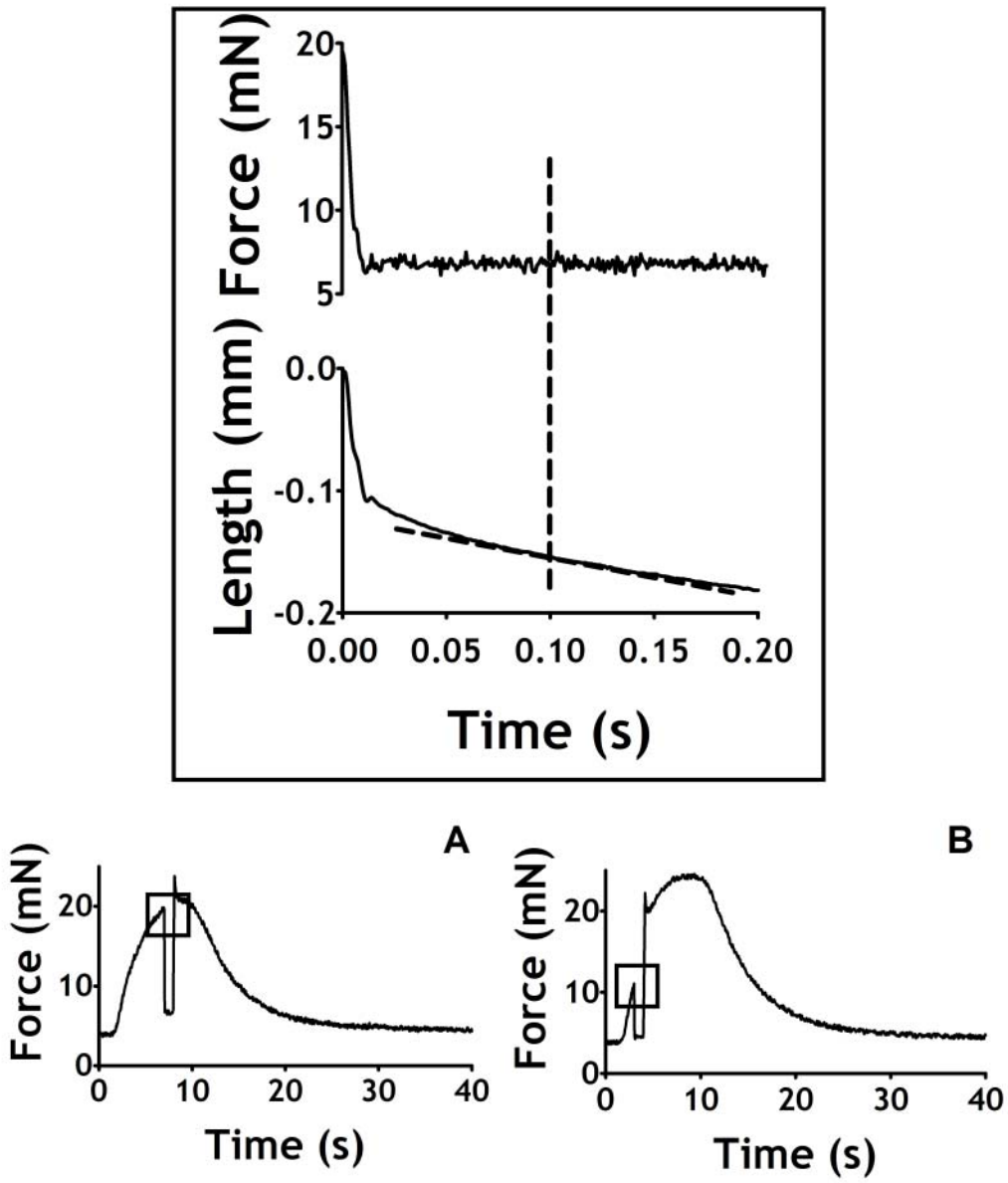

***Figure 6*. Isotonic shortening velocity measured against different loads at two time points.**

Isotonic shortening velocity was measured at five different loads both at the early and the late phase of contraction (refer to Fig. 5 for an example of shortening velocity measurement). The loads were determined as a percentage of F_{max}. Late release (black circles) and early release (grey triangles) data were fitted with Hill's hyperbolic equation. n=5 from 5 different donors. Late-phase $R^2 = 0.8665$, early-phase $R^2 = 0.8417$. The two groups were significantly different, repeated measures ANOVA: $p<0.0001$.

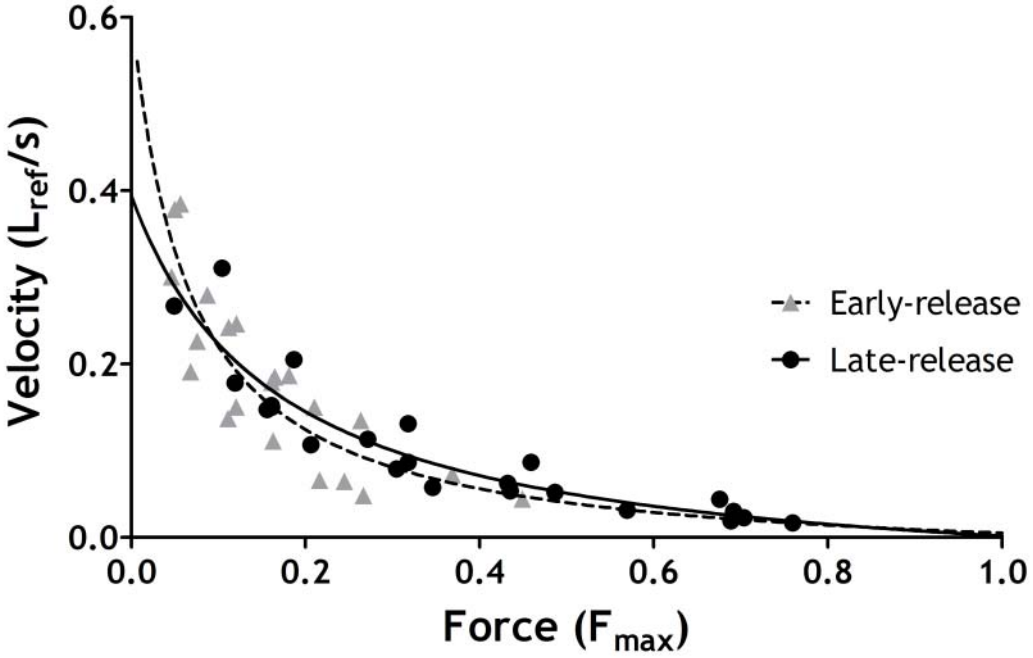

Figure 7. **Maximal Shortening**
ASM strips were stimulated to contract with EFS and the total amount of isotonic shortening against low loads was measured. Using the amount of shortening recorded at loads representing 10% and 20% of F_{max}, maximal shortening was extrapolated. Each symbol represents a muscle from a unique donor, n=4 from 4 different donors. R^2 = 0.7488, p=0.0055.

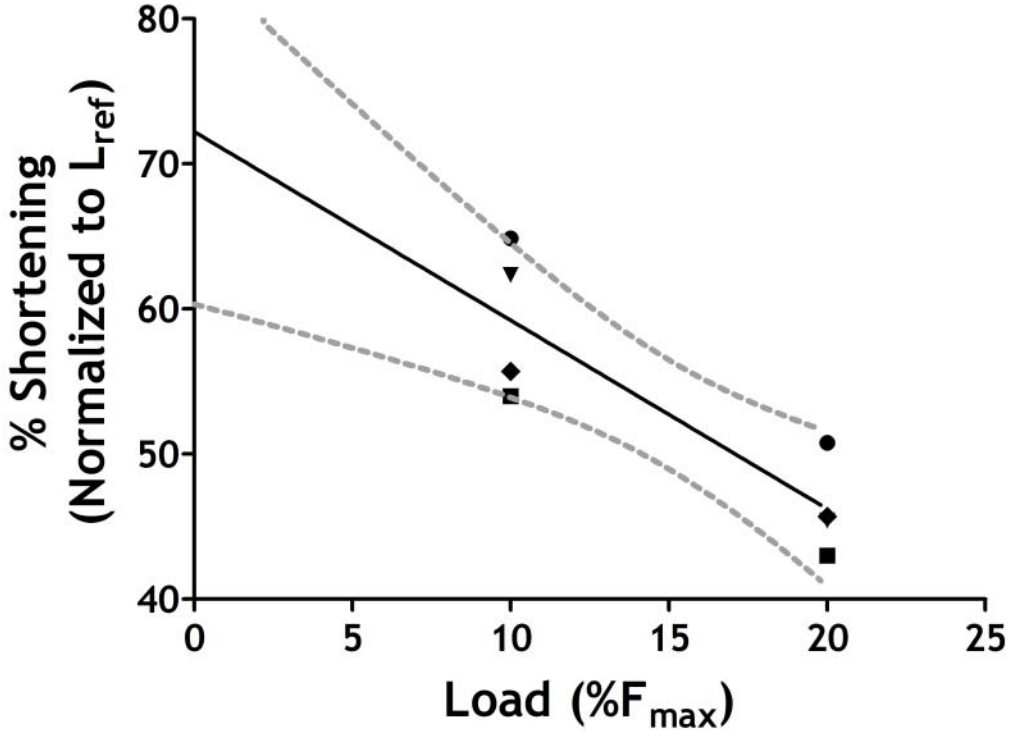
% Shortening
(Normalized to L_{ref})
80
70
60
50
40
0
5
10
15
20
25
Load (%F_{max})

Table 1. Subject demographics and clinical details.

Sex	Age	Weight (kg)	Height (cm)	Ethnicity	Cause of Death	Patient Medical History	Known Meds	Terminal Meds
M	4	17.5	104	Hispanic	Head trauma	None	None	Steroids and vasopressors
M	22	112	193	Caucasian	Head trauma	Occasional marijuana (once a year)	None	Vasopressors
F	63	77	159	Caucasian	Gastrointestinal bleed	Hypertension X 2 years	Unknown antihypertensive	Dopamine
F	19	87	165	Caucasian	Head trauma	None	None	Steroids and vasopressors
F	20	72.2	165	Caucasian	Head trauma	Smoked cigarettes < 1 PPD† for 2 years. Marijuana smoked unknown frequency.	Pain medications and inhalants	Vasopressors
M	24	81.8	175	Hispanic	Head trauma	None	None	Vasopressors

† Pack per day